

## Serum metabolomics analysis reveals increased lipid catabolism in mildly hyperbilirubinemic Gilbert's syndrome individuals



Claudia A. Hana<sup>a,\*</sup>, Lan V. Tran<sup>a</sup>, Christine Mölzer<sup>b</sup>, Elisabeth Müllner<sup>c</sup>, Marlies Hörmann-Wallner<sup>d</sup>, Bernhard Franzke<sup>a,e</sup>, Anela Tosevska<sup>a,f</sup>, Patrick A. Zöhrer<sup>a,e</sup>, Daniel Doberer<sup>g</sup>, Rodrig Marculescu<sup>h</sup>, Andrew C. Bulmer<sup>i</sup>, Heinz Freisling<sup>j</sup>, Ali A. Moazzami<sup>c,1</sup>, Karl-Heinz Wagner<sup>a,e,\*,1</sup>

<sup>a</sup> Faculty of Lifesciences, Department of Nutritional Sciences, University of Vienna, Vienna, Austria

<sup>b</sup> School of Medicine, Institute of Medical Sciences, Medical Sciences and Nutrition, University of Aberdeen, Aberdeen, United Kingdom

<sup>c</sup> Department of Molecular Sciences, Swedish University of Agricultural Sciences, Uppsala, Sweden

<sup>d</sup> Institute for Dietetics and Nutrition, University of Applied Sciences FH JOANNEUM, Graz, Austria

<sup>e</sup> Research Platform Active Ageing, University of Vienna, Vienna, Austria

<sup>f</sup> Internal Medicine III, Division of Rheumatology, Medical University of Vienna; Vienna, Austria

<sup>g</sup> Department of Clinical Pharmacology, Medical University of Vienna, Vienna General Hospital, Vienna, Austria

<sup>h</sup> Clinical Institute of Laboratory Medicine, Medical University of Vienna, Vienna General Hospital, Vienna, Austria

<sup>i</sup> School of Medical Science and Menzies Health Institute Queensland, Griffith University, Queensland, Australia

<sup>j</sup> Section of Nutrition and Metabolism, International Agency for Research on Cancer (IARC-WHO), Lyon, France

### ARTICLE INFO

#### Article history:

Received 8 July 2021

Accepted 7 October 2021

#### Keywords:

Bilirubin  
Metabolomics  
Lipid catabolism  
Ketone bodies  
Gilbert's syndrome

### ABSTRACT

**Background:** The protective role of mildly elevated bilirubin against CVD and diabetes mellitus type 2 (DMT2) is associated with a favorable lipid phenotype. As the mechanistic understanding of this protection in humans remains elusive, we aimed to assess the metabolomics profile of mildly hyperbilirubinemic (Gilbert's syndrome; GS) individuals especially targeting lipid catabolism.

**Methods and results:** Using NMR serum metabolomics of 56 GS individuals and 56 age and gender-matched healthy controls, GS individuals demonstrated significantly greater concentrations of acetylcarnitine (+20%,  $p < 0.001$ ) and the ketone bodies, 3-hydroxybutyric acid (+132%,  $p < 0.001$ ), acetoacetic acid (+95%,  $p < 0.001$ ) and acetone (+46%,  $p < 0.001$ ). Metabolites associated with an increased mitochondrial lipid metabolism such as citrate (+15%,  $p < 0.001$ ), anaplerotic amino acid intermediates and creatinine were significantly greater and creatine significantly reduced in GS individuals. Stimulators of lipid catabolism including AMPK (+59%,  $p < 0.001$ ), pPPAR $\alpha$  (+24%,  $p < 0.001$ ) and T3 (+9%,  $p = 0.009$ ) supported the metabolomics data while concomitantly blood glucose and insulin (−33%,  $p = 0.002$ ) levels were significantly reduced. We further showed that the increased lipid catabolism partially mediates the favorable lipid phenotype (lower triglycerides) of GS individuals. Increased trimethylamine (+35%,  $p < 0.001$ ) indicated changes in trimethylamine metabolism, an emerging predictor of metabolic health.

**Conclusion:** We showed an enhanced lipid catabolism in mildly hyperbilirubinemic individuals, novel evidence as to why these individuals are leaner and protected against chronic metabolic diseases emphasizing bilirubin to be a promising future target in obese and dyslipidemia patients.

© 2021 The Authors. Published by Elsevier Inc. This is an open access article under the CC BY license (<http://creativecommons.org/licenses/by/4.0/>).

### 1. Introduction

Diabetes mellitus type 2 (DMT2) and cardiovascular diseases (CVD) are reaching epidemic proportions worldwide, affecting all socioeconomic backgrounds and ethnicities [1–3]. Key factors in the etiology

of DMT2 and CVD include obesity, hyperlipidemia and glucose intolerance [4,5]. Today, a vast body of evidence indicates that mildly elevated circulating bilirubin is a protective factor against obesity, high blood lipids and insulin resistance [6–12] and is inversely associated with the risk of DMT2 and CVD [13–16].

Individuals with Gilbert's syndrome (GS), a benign condition with a prevalence of 2–10% among Caucasians, are diagnosed based on their chronically mildly elevated unconjugated bilirubin (UCB) levels [17]. These mildly increased UCB levels are associated with mutations within the uridine diphosphate glucuronosyltransferase 1A1 (UGT1A1) such as

\* Corresponding authors at: University of Vienna, Department of Nutritional Sciences, Althanstraße 14, 1090 Vienna, Austria.

E-mail addresses: [claudia.hana@univie.ac.at](mailto:claudia.hana@univie.ac.at) (C.A. Hana),

[karl-heinz.wagner@univie.ac.at](mailto:karl-heinz.wagner@univie.ac.at) (K.-H. Wagner).

<sup>1</sup> These authors contributed equally to this work.

**Abbreviations**

AC	acetylcarnitine
AMPK	5' AMP-activated protein kinase
CVD	cardiovascular diseases
DMT2	type 2 diabetes mellitus
FAO	fatty acid oxidation
FMO3	flavin-containing monooxygenase 3
GS	Gilbert's syndrome
HOMA-IR	homeostatic model assessment for insulin resistance
KB	ketone bodies
PBMCs	peripheral blood mononucleated cells
PGC1 $\alpha$	peroxisome proliferator-activated receptor gamma co-activator 1-alpha
PPAR $\alpha$	peroxisome proliferator-activated receptor alpha
TCA	tricarboxylic acid cycle
TG	triglycerides
TH	thyroid hormones
TMA	trimethylamine
TMAO	trimethylamine N-oxide
UGT1A1	uridine diphosphate glucuronosyltransferase 1A1

the GS-associated UGT1A1\*28 (TA)<sub>6>7</sub> insertion polymorphism leading to a decreased expression of the UGT1A1 enzyme and to a reduced UCB clearance [18,19]. Furthermore, GS individuals have a favorable lipid phenotype including reduced blood lipids, fat mass and BMI [20,21] and are unique human models to study protective effects of the bilirubin metabolism in humans. In a previous study, we have been able to associate the GS with increased phosphorylation of AMPK and PPAR $\alpha$ , two established stimulators of lipid and energy metabolism [22]. To this date, the mechanistic understanding of bilirubin's protective function in humans, remains otherwise largely elusive.

To fill this gap, this study aimed to identify a GS-specific metabolic profile using NMR-metabolomics. We were particularly targeting

downstream metabolites of ketogenesis and fatty acid oxidation (FAO) and further investigated associations with circulating and leukocyte expressed metabolic regulators (insulin, glucagon, thyroid hormones (TH), catecholamines, AMPK, PPAR $\alpha$ ) to understand their potential interaction in influencing lipid catabolism in GS individuals. We hypothesized that lipid catabolism would be increased in GS individuals, compared to controls.

**2. Material and methods****2.1. Study design and participants**

The BiliHealth study (Fig. 1) was an observational age and gender matched case-control study performed at the Department of Clinical Pharmacology at the Vienna General Hospital. Subjects were recruited between June 2014 and January 2015, from the department's subject database and by advertising through posters and flyers. To challenge metabolism all participants had to complete a 400 kcal/d fasting protocol and an overnight fast of 16 ( $\pm$ 1) hours before blood sampling. GS individuals had to meet the following criteria to be included into the study [23]. Their fasted UCB levels in serum had to be equal to, or higher than, the diagnostic clinical UCB threshold for GS of 17.1  $\mu$ M UCB (corresponds to  $\sim$ 1.2 mg/dL total bilirubin) at two individual time points. Liver disease was excluded on the basis of normal aspartate aminotransferase (AST), alanine transaminase (ALT), gamma-glutamyl transferase (GGT) and lactate dehydrogenase (LDH) (Table S1). GS and control subjects had to be healthy adults (>20 or <80 years) with no medical history of any acute and chronic (metabolic/inflammatory) diseases and a moderate level of physical activity. Further exclusion criteria included smoking, professional athletes, overt hemolysis, intake of antioxidants or liver influencing medication within the last 5 weeks before the study, cholelithiasis, pregnancy, present or past neoplasia and organ transplants. The study was approved by the Ethics Commission of the Medical University of Vienna (No. 1164/2014) and was conducted in accordance with the approved guidelines by the Declaration of Helsinki. Written informed consent was received prior to participation.

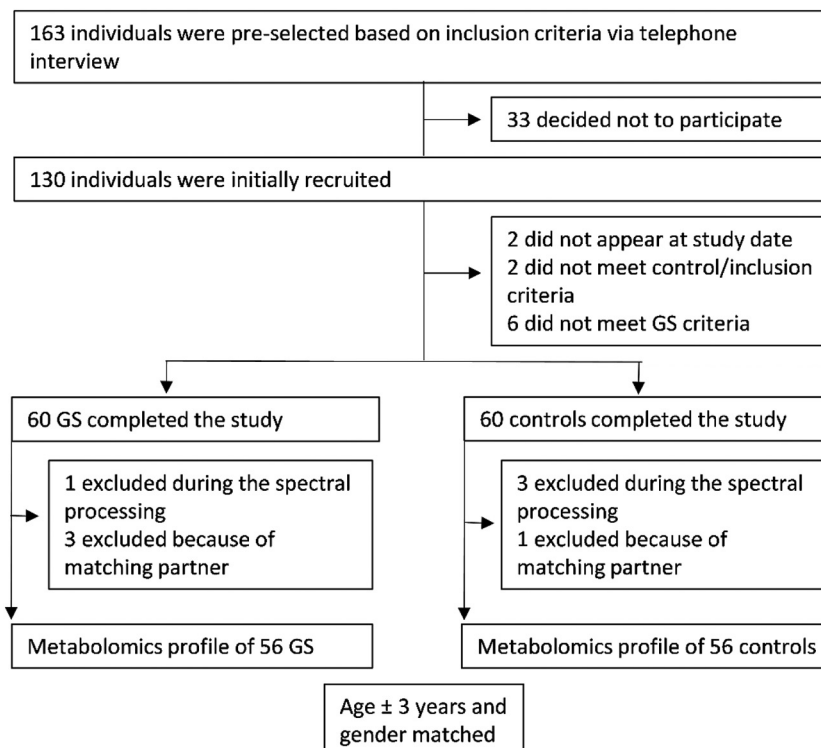


Fig. 1. Flow chart of the BiliHealth study.

## 2.2. Blood biochemistry

Fasted venous blood samples were collected by venipuncture into serum, EDTA and Li-Heparin Vacutainers (Z Serum Sep, K2EDTA and Li-Heparin, respectively). Samples were cooled, protected from light and immediately analyzed. For future analysis, aliquoted samples were stored at  $-80^{\circ}\text{C}$ . Glucose, insulin, C-peptide, glucagon, HbA1c, triglycerides (TG), total cholesterol, HDL, LDL, normetanephrine, metanephrine, Thyroid-stimulating hormone (TSH), triiodothyronine (T3), thyroxine (T4), total bilirubin, AST, ALT, GGT and LDH were analyzed in the central laboratories of the Vienna General Hospital (Olympus 5400 clinical chemistry analyzers, Beckman Coulter) on the day of blood sampling. Insulin resistance was calculated using homoeostasis model assessment [(fasted insulin [ $\mu\text{U}/\text{mL}$ ]  $\times$  fasted blood glucose [ $\text{mg}/\text{dL}$ ])/405]. Serum UCB was measured by an in-house HPLC method [24] and genotyping of the *UGT1A1* was performed as described elsewhere [22,25]. AMPK, PPAR $\alpha$  and PGC1 $\alpha$  were analyzed in antibody stained peripheral blood mononucleated cells (PBMCs) using flow cytometry by Mölzer et al. [22]. The following antibody set-up was used: rabbit anti-human monoclonal to AMPK  $\alpha$ 1 (phos-T183) and AMPK  $\alpha$ 2 (phos-T172) (ab133448, Abcam) and secondary antibody: goat anti-rabbit IgG H & L AlexaFluor 488 (ab150077, Abcam); rabbit anti-human polyclonal to PGC1 $\alpha$  PE-labelled (orb124814, Biorbyt) and rabbit anti-human polyclonal to PPAR $\alpha$  (phos-Ser12) FITC-labelled (bs-4055R-FITC, Bioss).

## 2.3. Anthropometric measurements

Body weight was measured in the morning of the study day to the nearest 0.1 kg barefoot and lightly dressed, height was assessed to the nearest 0.5 cm without shoes and BMI ( $\text{kg}/\text{m}^2$ ) was calculated. Waist circumference (WC) and hip circumference (HC) were measured by tape (model 203, Seca) held snugly at a level parallel to the floor. WC was measured as the narrowest circumference between the lower rib margin and anterior superior iliac crest. HC around the widest portion of the buttocks, and the waist-to-hip (WHR) ratio was calculated. Fat mass and lean body mass were measured by Bioelectric Impedance Analysis (BIA) in the morning of the study day using a BIA Analyzer 2000-S (Data-Input GmbH, Darmstadt, Germany). Food consumption was reported using a food frequency questionnaire as described previously [22]. In addition, all participants were required to answer questions about frequency of physical activity including everyday activity such as walking and climbing stairs as well as endurance and strength exercise of at least 30 min per week, as has been published recently [22].

## 2.4. NMR serum metabolomics

Metabolomics analyses were performed by  $^1\text{H}$  NMR at the Swedish University of Agricultural Sciences in Uppsala. Samples were prepared for NMR analysis according to Moazzami et al. [26] with slight modifications [26]. Briefly, serum samples were slowly thawed on ice and ultrafiltration was used to remove plasma proteins in each sample. Filters with a 3 kDa cut-off (Amicon® filter Merck Millipore Ltd., Billerica, Massachusetts) were used. The filters were washed once with water (9 mL,  $36^{\circ}\text{C}$ , 1500 g, 2 h) prior to sample filtration (400  $\mu\text{L}$  serum,  $4^{\circ}\text{C}$ , 10,000 g, 155–180 min) to remove the glycerol from the filter membrane. The sample solutions for the  $^1\text{H}$ -NMR analysis consisted of 310  $\mu\text{L}$  of the serum sample filtrate, 150  $\mu\text{L}$  phosphate buffer (0.4 M, pH 7.0), 65  $\mu\text{L}$  water, 45  $\mu\text{L}$   $\text{D}_2\text{O}$  and 30  $\mu\text{L}$  of the internal standard trimethyl-silyl-d-4-propionic acid (TSP) (5.8 mM). 560  $\mu\text{L}$  of each sample solution was transferred to a 5 mm NMR tube. For a second batch a scaled down protocol of the same method was used according to Röhnisch et al. [27] due to sample availability. Briefly, 60  $\mu\text{L}$  serum was extracted at  $4^{\circ}\text{C}$ , 13,000 g using Nanosep centrifugal filters (Pall Life Science) and 170  $\mu\text{L}$  sample solution (40  $\mu\text{L}$  serum filtrate, 50  $\mu\text{L}$  phosphate buffer, 55  $\mu\text{L}$  water, 15  $\mu\text{L}$   $\text{D}_2\text{O}$  and 10  $\mu\text{L}$  TSP) were transferred to a 3 mm NMR tube. The GS and the corresponding matched control samples were always analyzed

pairwise using the same methodology and NMR conditions. For  $^1\text{H}$  NMR spectrum acquisition, a Bruker Avance III spectrometer operating at 600 MHz proton frequency, equipped with a cryogenically cooled probe and an autosampler was used. The spectra were recorded at  $25^{\circ}\text{C}$  using 128 scans (512 scans for 3 mm tubes) and 4 s relaxation delay with a zgsgp pulse sequence (Bruker Biospin). For each spectrum 65,536 data points were collected over a spectral width of 17,942 Hz. The spectral quality was assessed immediately after acquisition, based on the shape of the internal TSP signal using a line broadening factor of 0.3 Hz to ensure that full-width, halfmaximum (FWHM) was  $<1.0$  Hz. The  $^1\text{H}$  NMR spectra were processed manually with the NMR Suite Professional Software package (version 7.5; ChenomX Inc., Edmonton, Canada) including phase correction, baseline correction and line broadening. Identification and quantification of the metabolites was performed according to a previously published method by Röhnisch et al. [27]. 58 metabolites were identified using the NMR Suite 8.3 library, the Biological Magnetic Resonance Data Bank and the Human Metabolome Data Base and were quantified using the Automated Quantification Algorithm Aqua [27]. The final serum sample concentrations considered the dilution factor and statistical analysis

**Table 1**  
Baseline and metabolic characteristics of GS and control individuals.

	Gilbert's syndrome		Control		p-Value	n (GS)	n (C)
Subjects	56		56				
Median age [yrs]	31.5	18.8	32.5	18.0	0.233	56	56
Male/female [n]	36/20		36/20				
UCB concentration [ $\mu\text{M}$ ]	32.58	16.21	8.90	5.37	<b>0.000</b>	56	56
Health food [t/w] <sup>o</sup>	30.0	8.5	27.0	12.0	0.268	42	47
Snack food [t/w]	9.0	9.0	11.0	8.8	0.863	43	52
Red meat [t/w]	2.0	5.0	3.0	5.0	0.405	43	52
Alcohol [t/w]	0.0	4.0	0.0	2.0	0.235	43	48
Overall activity [t/w] <sup>o</sup>	5.9	2.7	6.2	3.4	0.615	54	49
Resistance exercise [t/w]	1.0	2.0	0.3	2.0	0.739	54	49
Endurance exercise [t/w] <sup>o</sup>	2.8	1.9	3.3	2.4	0.311	55	55
BMI [ $\text{kg}/\text{m}^2$ ] <sup>o</sup>	22.76	2.93	25.44	4.96	<b>0.001</b>	56	56
Body size [ $\text{cm}$ ] <sup>o</sup>	179.0	14.0	176.5	17.0	0.119	56	56
Body weight [ $\text{kg}$ ] <sup>o</sup>	71.38	13.87	77.80	17.75	<b>0.011</b>	56	56
WC [ $\text{cm}$ ] <sup>o</sup>	79.62	10.30	86.68	15.99	<b>0.003</b>	56	56
HC [ $\text{cm}$ ] <sup>o</sup>	94.23	6.48	99.79	9.36	<b>0.001</b>	56	56
WHR <sup>o</sup>	0.84	0.07	0.86	0.10	0.083	56	56
LBM [%] <sup>o</sup>	78.15	6.43	74.77	8.50	<b>0.024</b>	55	54
LBM [ $\text{kg}$ ] <sup>o</sup>	55.67	9.41	57.08	12.21	0.156	55	54
Body fat [%] <sup>o</sup>	21.85	6.43	25.23	8.50	<b>0.024</b>	55	54
Body fat [ $\text{kg}$ ] <sup>o</sup>	16.07	6.70	19.88	9.71	<b>0.023</b>	55	54
Systolic bp, [mm Hg] <sup>o</sup>	130.43	13.20	132.28	16.11	0.515	54	54
Diastolic bp, [mm Hg] <sup>o</sup>	67.22	12.02	68.81	12.13	0.495	54	54
Intermediate bp [mm Hg] <sup>o</sup>	99.11	11.04	100.81	12.30	0.450	54	54
MAP [mm Hg] <sup>o</sup>	108.94	11.39	110.70	13.27	0.460	54	54
TSH [ $\mu\text{U}/\text{mL}$ ] <sup>o</sup>	1.94	0.96	2.07	1.00	0.537	55	55
T3 [pg/mL] <sup>o</sup>	1.34	0.25	1.23	0.15	<b>0.009</b>	55	55
T4 [ng/dL] <sup>o</sup>	3.21	0.48	3.19	0.37	0.937	55	55
T3/T4 ratio <sup>o</sup>	0.41	0.01	0.39	0.01	0.137	55	55
Metanephrine [pg/mL]	22.68	24.71	20.17	15.88	0.613	56	56
Normetanephrine <sup>o</sup> [pg/mL]	52.51	26.47	49.07	32.13	0.551	56	56
Glucose [mg/dL] <sup>o</sup>	81.60	7.32	85.89	7.99	<b>0.006</b>	55	56
Insulin [ $\mu\text{U}/\text{mL}$ ]	4.10	2.40	6.10	6.10	<b>0.002</b>	55	55
C-peptide [ng/mL]	1.20	0.50	1.50	1.10	<b>0.001</b>	55	55
Glucagon [pg/mL] <sup>o</sup>	17.29	10.06	17.49	12.87	0.924	56	56
HOMA-IR	0.81	0.53	1.27	1.28	<b>0.001</b>	54	55
HbA1c [%] <sup>o</sup>	4.96	0.36	5.08	0.37	0.062	56	56
Triglycerides [mg/dL] <sup>o</sup>	74.79	30.82	93.43	44.41	<b>0.007</b>	53	56
T-chol. [mg/dL] <sup>o</sup>	174.22	36.36	187.73	41.13	0.054	54	56
HDL chol. [mg/dL] <sup>o</sup>	66.07	19.82	63.30	18.93	0.333	54	56
LDL chol. [mg/dL] <sup>o</sup>	92.77	33.26	105.74	38.18	<b>0.048</b>	54	56
LDL/HDL ratio <sup>o</sup>	1.55	0.77	1.89	1.09	<b>0.046</b>	54	56

Data are provided as median/IQR, mean/ $\text{SD}^{\circ}$  or n. Boldface indicates significant  $p$  values  $\leq 0.05$ . Health food consumption: rich in vitamins, antioxidants, unsaturated fatty acids and fibres. Snack food consumption: fatty and sugary snacks. Overall activity: climbing stairs, walking, resistance exercise and endurance exercise of at least 30 min, [t/w] = [times/week], LBM: lean body mass, WC: waist circumference, HC: hip circumference, bp = blood pressure, MAP: mean arterial pressure, t-chol: total cholesterol.

was performed with 51 metabolites that were above the limit of detection [27].

### 2.5. Statistical analysis

Comparison of GS and control individuals was performed using paired *t*-test (for parametric distribution) or Wilcoxon signed-rank test (for non-parametric distribution) restricted to participants with no missing data. Data distribution was assessed based on histograms. For metabolomics analyses, *p*-values were corrected for false discoveries [28] using the *qvalue* R package in R version 3.1.2. Descriptive statistics are reported as mean ( $\pm$ SD) or median (IQR) and considered the number of participants per variable and group as shown in Tables 1, 2 and 3. Pre-specified bivariate correlations between lipid catabolites and (1) metabolic regulators (AMPK, PPAR $\alpha$ , insulin, glucagon, and catecholamines), (2) fasting biomarkers and (3) risk factors of chronic diseases were modelled using Pearson or Spearman-Rho. The correlation plots were generated using the *ggcorrplot* package in R version 4.0.3. Linear regressions were modelled with circulating TG as dependent variable and GS-status and lipid catabolites as independent variables. Calculations were completed using SAS 9.4 (SAS Institute Inc., North Carolina, USA) and IBM SPSS 24 (IBM Corp. IBM SPSS Statistics for Windows, NY, USA). Unless otherwise specified *p*  $\leq$  0.05 (two-sided) was considered significant.

## 3. Results

### 3.1. Baseline and metabolic characteristics: favorable metabolic biomarkers but similar life-style in GS individuals

There were 112 participants (56 GS and 56 control individuals) with complete metabolomics data in the study (Fig. 1). Individuals in the GS and control group had a similar age distribution, food consumption and physical activity. In contrast to controls, as expected, GS individuals had mild unconjugated hyperbilirubinemia (Table 1) but all hepatic parameters were within normal ranges in both groups (Table S1). In accordance to literature, GS individuals presented either a homozygous (*n* = 25), heterozygous (*n* = 26) or no (*n* = 3) UGT1A1\*28 (TA)<sub>6>7</sub> insertion polymorphism (Table S1) showing that this mutation is associated with GS but not sufficient for its manifestation [18,29].

Subjects with GS exhibited significantly reduced fat mass ( $-13\%$ , *p* = 0.024), BMI ( $-10\%$ , *p* = 0.001), blood triglycerides (TG) ( $-20\%$ , *p* = 0.007), LDL-Cholesterol ( $-12\%$  *p* = 0.048) and LDL/HDL ratio ( $-18\%$ , *p* = 0.046). Similarly, The GS glucose metabolic phenotype demonstrated lower fasting glucose ( $-5\%$ , *p* = 0.006), insulin ( $-33\%$ , *p* = 0.002), HOMA-IR ( $-36\%$ , *p* = 0.001), C-peptide ( $-20\%$ , *p* = 0.001) and a trend towards reduced HbA1c ( $-2\%$ , *p* = 0.062) (Table 1) compared to non-GS subjects.

### 3.2. GS-specific metabolites in the NMR-metabolomics profile

We quantified 58 metabolites using NMR. Concentrations of these metabolites in the GS vs. the control group are shown in Table 2. After correction for false discoveries, the concentration of 16 metabolites was significantly different between the groups.

### 3.3. Increased concentrations of acetylcarnitine (AC) and ketone bodies (KB) in GS individuals

The AC concentration was significantly greater ( $+20\%$ , *p* < 0.001) in the serum of GS compared to control individuals. Simultaneously, 3-hydroxybutyric acid (3HB) ( $+132\%$ , *p* < 0.001), acetoacetic acid (AcAc) ( $+95\%$ , *p* < 0.001) and acetone (Ac) ( $+46\%$ , *p* < 0.001) levels were all significantly increased in the serum of GS subjects (Table 2). We observed strong and significant correlations between AC and the three KBs (e.g.

**Table 2**  
Metabolomics profile of GS and control individuals.

Metabolites	%Change to control	Gilbert's syndrome		Control	p-Value	
3-Hydroxybutyric a.	132.47	207.60	84.60	89.30	44.18	0.000
Acetone	46.09	23.99	25.20	16.42	8.24	0.000
Trimethylamine	35.41	2.13	1.49	1.58	1.22	0.000
Acetylglycine	20.32	8.26	6.73	6.86	2.98	0.000
Citric a.	14.67	149.84	46.09	130.68	39.58	0.000
Acetylcarnitine	20.47	12.03	5.82	9.99	4.79	0.000
2-Oxoisocaproic a.	12.01	8.90	5.36	7.95	3.92	0.001
Acetoacetic a.	94.83	55.24	71.16	28.36	46.58	0.001
Glutamine	6.88	443.74	122.99	415.19	75.64	0.002
2-Hydroxybutyric a.	27.55	50.23	43.32	39.38	27.04	0.002
Creatine	-19.73	15.28	10.69	19.03	17.81	0.003
Leucine	10.74	124.85	48.15	112.75	32.93	0.005
2-Aminobutyric a.	12.54	29.34	13.27	26.07	10.74	0.007
2-Ketoglutaric a.	2.19	12.07	6.30	11.81	4.25	0.009
Creatinine	4.54	74.61	20.46	71.36	20.37	0.013
Histidine	1.99	79.98	27.33	78.42	17.64	0.018
3-Hydroxyisovaleric a.	3.66	2.44	0.31	2.35	0.22	0.023
Tyrosine <sup>a</sup>	-6.57	57.34	11.38	61.38	12.11	0.037
Myoinositol	5.03	32.61	9.24	31.05	6.96	0.044
Dimethylsulfone	-27.85	3.18	2.99	4.41	3.24	0.044
Methanol	39.04	362.92	772.76	261.01	774.68	0.056
Glycine	11.18	228.00	90.41	205.07	76.30	0.062
Proline	-10.23	162.69	57.65	181.22	63.66	0.089
Asparagine	0.33	52.60	14.88	52.42	11.81	0.090
Glucose	-5.34	3062.40	788.59	3235.18	777.63	0.107
2-Hydroxyisovaleric a.	3.76	9.06	5.68	8.74	5.17	0.111
Acetic a.	10.87	40.01	14.60	36.09	20.45	0.111
Lysine	2.46	156.08	54.00	152.33	44.98	0.133
Betaine	-3.60	35.81	11.78	37.15	12.68	0.152
Pyruvic a.	9.59	59.86	25.10	54.63	24.59	0.161
Valine	3.77	237.42	17.54	228.81	11.98	0.192
Methionine	-0.12	28.97	8.61	29.00	7.19	0.216
Dimethylglycine	3.19	3.16	1.28	3.07	1.40	0.253
Isoleucine <sup>a</sup>	3.67	66.76	16.56	64.40	14.51	0.266
Ophosphocholine	-6.33	2.17	1.22	2.31	1.32	0.282
TMAO <sup>a</sup>	6.16	31.53	10.95	29.70	8.79	0.310
Formic a.	-6.49	16.14	6.16	17.26	6.88	0.439
Choline	7.46	10.51	3.70	9.78	3.18	0.459
Ornithine <sup>a</sup>	3.42	58.20	16.10	56.27	15.42	0.504
Alanine	-1.38	330.39	92.45	335.00	98.25	0.653
Butyrate	19.76	6.84	5.75	5.72	5.78	0.664
Carnitine	3.87	38.69	14.70	37.25	10.13	0.674
Glutamic a.	15.40	47.92	21.95	41.53	27.87	0.676
Threonine <sup>a</sup>	-1.38	121.82	25.21	123.52	22.01	0.683
Arginine	2.71	96.67	53.24	94.12	38.68	0.741
Glycerol	-7.71	679.20	361.87	735.96	336.69	0.747
Lactic a.	1.10	1849.84	517.79	1829.75	572.55	0.772
Ethanol	24.36	40.97	241.68	32.94	141.73	0.847
Phenylalanine	-2.58	48.62	10.16	49.91	8.76	0.847
Succinic a.	-1.14	7.67	3.17	7.75	3.24	0.877
Serine	1.84	130.35	42.99	127.99	35.16	0.962

Concentrations are provided in  $\mu$ M, data are median/IQR or mean/SD<sup>a</sup>. P-values were determined using paired *t*-test or Wilcoxon signed-rank test, metabolites above the red line had a *q*-value  $\leq$  0.05 after correction for false discoveries, *n* = 56 in the GS and control group respectively (creatine, tyrosine and acetic acid *n* = 55 per group), a.:acid, TMAO: Trimethylamine N oxide.

AC vs. 3HB *r* = 0.741, *p* < 0.001) in the GS and the whole study population (Fig. 2B).

### 3.4. GS metabolomics profile and mitochondrial lipid metabolism

In addition to AC and KB (end products of the mitochondrial FAO), we found significantly greater concentrations of citrate ( $+15\%$ , *p* < 0.001), a cataplerotic TCA-cycle intermediate in GS individuals. The anaplerotic TCA-cycle intermediates 2-aminobutyric acid ( $+13\%$ , *p* = 0.007), 2-hydroxybutyric acid ( $+28\%$ , *p* = 0.002) and 2-ketoglutaric acid ( $+2\%$ , *p* = 0.009) [30] were significantly increased and correlated significantly with their respective parent amino acids (Fig. 3). Further, creatine was significantly decreased ( $-20\%$ , *p* = 0.003) and creatinine

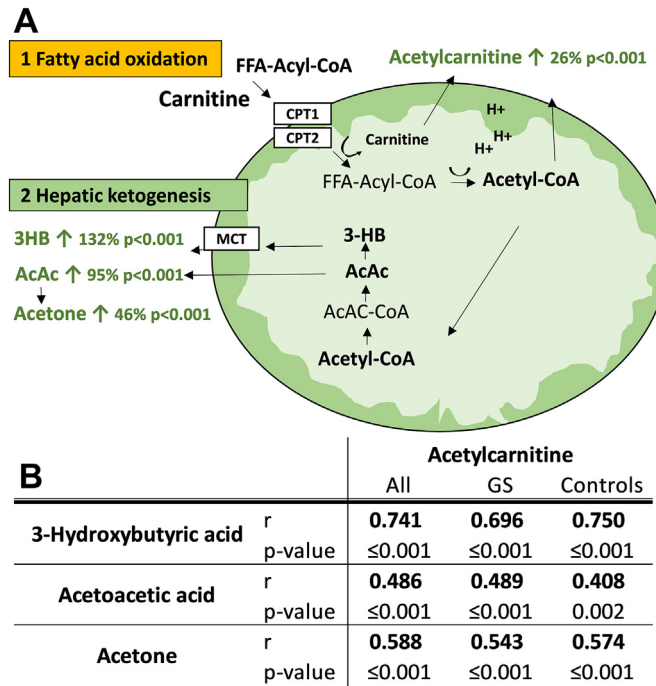


**Fig. 2.** GS metabolomics profile and lipid catabolism. (A) Schematic representation of a liver mitochondria shows hepatic FAO and ketogenesis as well as AC and KBs, their respective end products. Significantly increased ↑ metabolites (%) and p-values of GS compared to control individuals are in green. CPT1/2: Carnitine palmitoyl-transferase 1/2, MCT: monocarboxylate transporters. (B) Correlations of AC with KBs in the entire study population (all) as well as in GS and controls individually using Pearson or Spearman-Rho.

significantly increased (+5%,  $p = 0.013$ ) in GS serum, both being intermediates of the mitochondrial creatine phosphate shuttle. A schematic description of these metabolites and their associations with mitochondrial lipid metabolism is depicted in Figs. 2 and 3.

3.5. PPARα and pAMPK are significantly correlated with AC and KB serum levels

Abundance of the active, phosphorylated forms of AMPK ( $\alpha 1$  T183 and  $\alpha 2$  T172), PPARα (Ser12) and PGC-1α were significantly increased

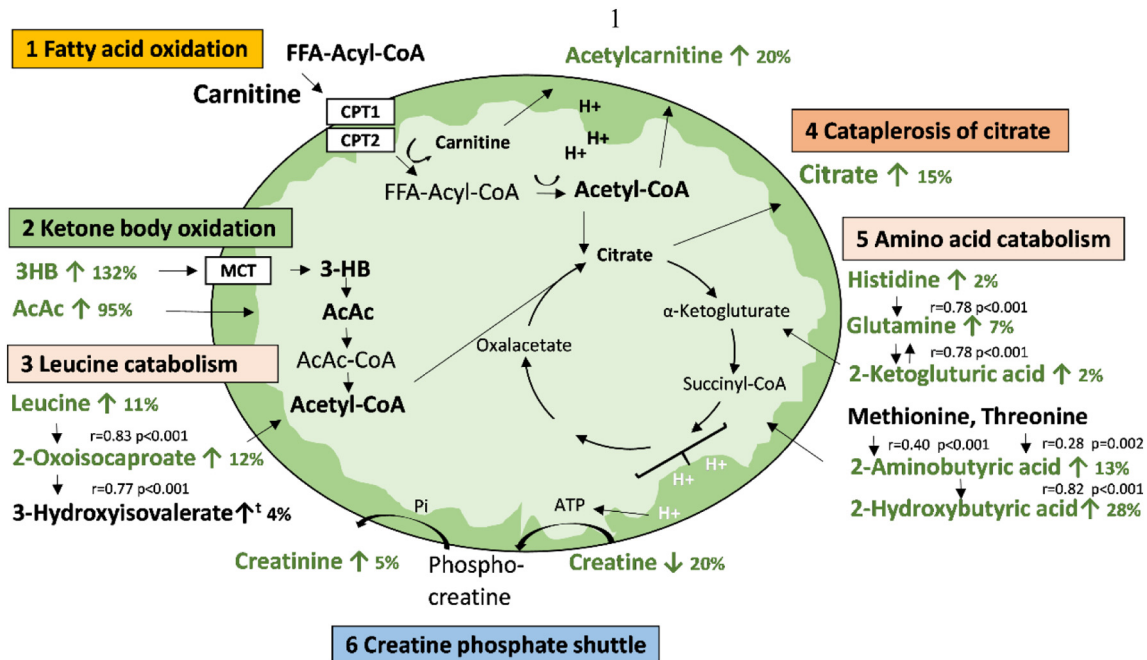


**Fig. 3.** GS metabolomics profile and mitochondrial lipid metabolism, a schematic representation. Cataplerosis of citrate (4) occurs as a response to an increased acetyl-CoA flux into the TCA-cycle, mainly derived from mitochondrial FAO (1) or KB-oxidation (2) under fasting conditions. To sustain TCA activity at this rate, anaplerotic replenishment with amino acid intermediates (5) is essential [23]. Creatine (6) functions as mitochondrial phosphate shuttle during increased mitochondrial ATP production. Significantly increased ↑ or decreased ↓ metabolites (%) in GS individuals compared to controls are in green. t = trend after false discoveries correction. Correlation coefficients (r) and p-values are presented between respective amino acids and their intermediates.

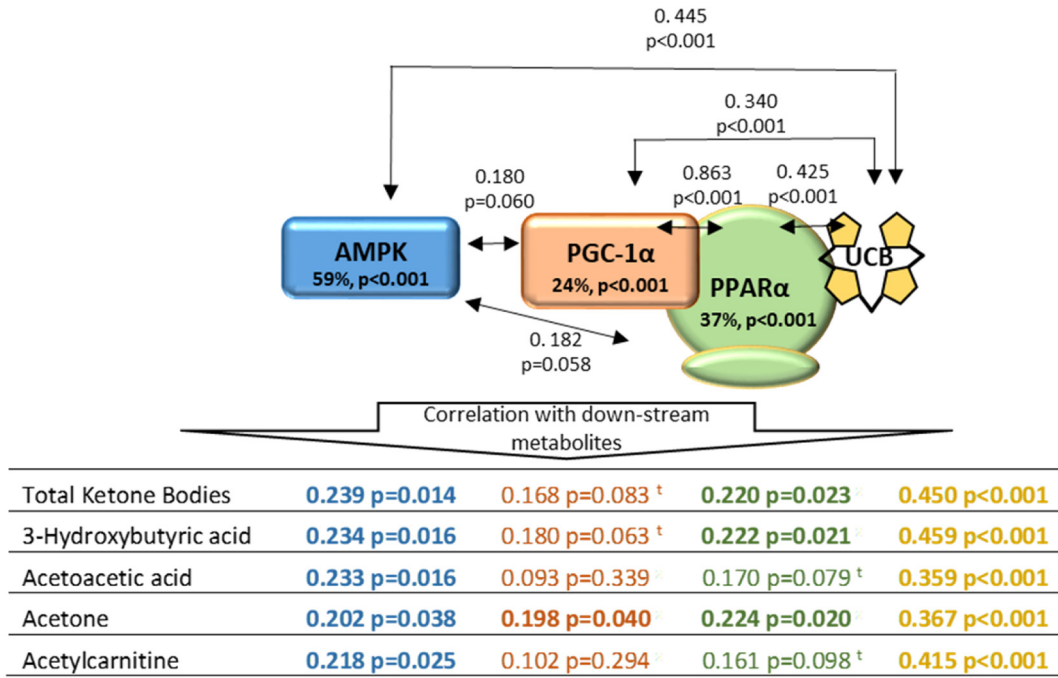


**Fig. 4.** AMPK, PPARα, PGC1α and lipid catabolism. The figure presents the % increase of AMPK, PPARα and PGC-1α measured in PBMCs of GS vs. control individuals, as previously published by Mólzer et al. [22] and correlation coefficients (r) between UCB, AMPK; PPARα and PGC-1 α. The table shows correlations coefficients and p-values of AMPK (blue), PGC1α (orange), PPARα (green) and UCB (yellow) with their downstream lipid metabolites in the whole study population using Pearson or Spearman-Rho. Significant correlations are in bold type, † = trend.

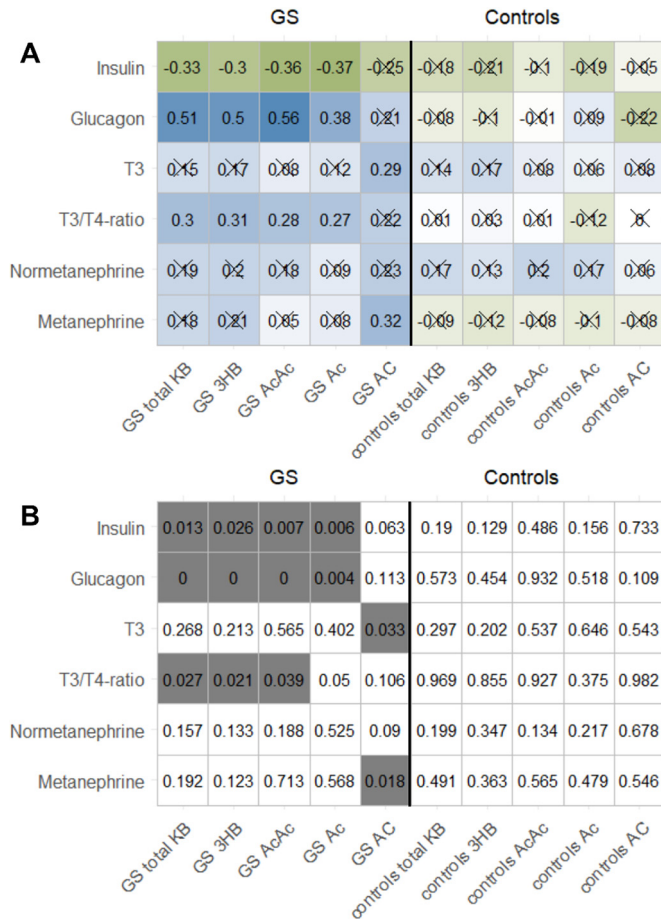


**Fig. 5.** Insulin, glucagon, THs and lipid catabolism. (A) Correlation coefficients (r) of hormonal regulators of lipid catabolism with KB and AC in the GS and control group. Positive correlations are in blue and negative in green using Pearson or Spearman-Rho. Crosses indicate non-significant correlations (p > 0.05). (B) Corresponding p-values, 0: p < 0.001.

in PBMCs of GS individuals compared to controls, as published previously in the same cohort [22]. In the present investigation, pAMPK and pPPAR $\alpha$  were significantly associated with their downstream metabolites AC, 3HB, AcAc and Ac in serum (Fig. 4).

3.6. Hormonal key players support the metabolomics profile in GS individuals

To explore a potential hormonal metabolic regulation of lipid catabolism in GS individuals, we analyzed TH, catecholamines, glucagon and insulin and explored their associations with AC and KB. Insulin and T3 differed significantly between GS individuals and controls (Table 2). Furthermore, correlation analysis revealed significant associations exclusively in the GS group (Fig. 5). In detail, insulin correlated negatively with the lipid catabolites while glucagon, T3 and the T3/T4 ratio, stimulators of lipid catabolism, were positively correlated with lipid catabolites in GS individuals.

3.7. The role of lipid catabolism in the bilirubin-associated protection against DMT2 and CVD

We correlated metabolites of lipid catabolism with circulating TG, LDL, body fat, HOMA-IR and C-peptide, all of which are major risk factors of DMT2 and CVD [2,31,32]. Lipid catabolites were inversely associated with these risk factors exclusively in GS individuals (Fig. 6). We further aimed to investigate whether the effect of GS on circulating TG is mediated through increased lipid catabolism, because circulating TG are a major source for lipid oxidation. We performed linear regressions with circulating TG as dependent and GS-status as well as KB, AC and citrate as independent variables. KB, AC and citrate were used as a measure of lipid catabolism as they are formed by acetyl-groups that abundantly accumulate during lipid oxidation (see Figs. 2 and 3). After adjustment for these lipid catabolites, associations between GS-status and circulating TG were attenuated by up to 36% and were no longer significant ( $p = 0.185$ ) (Fig. 7).

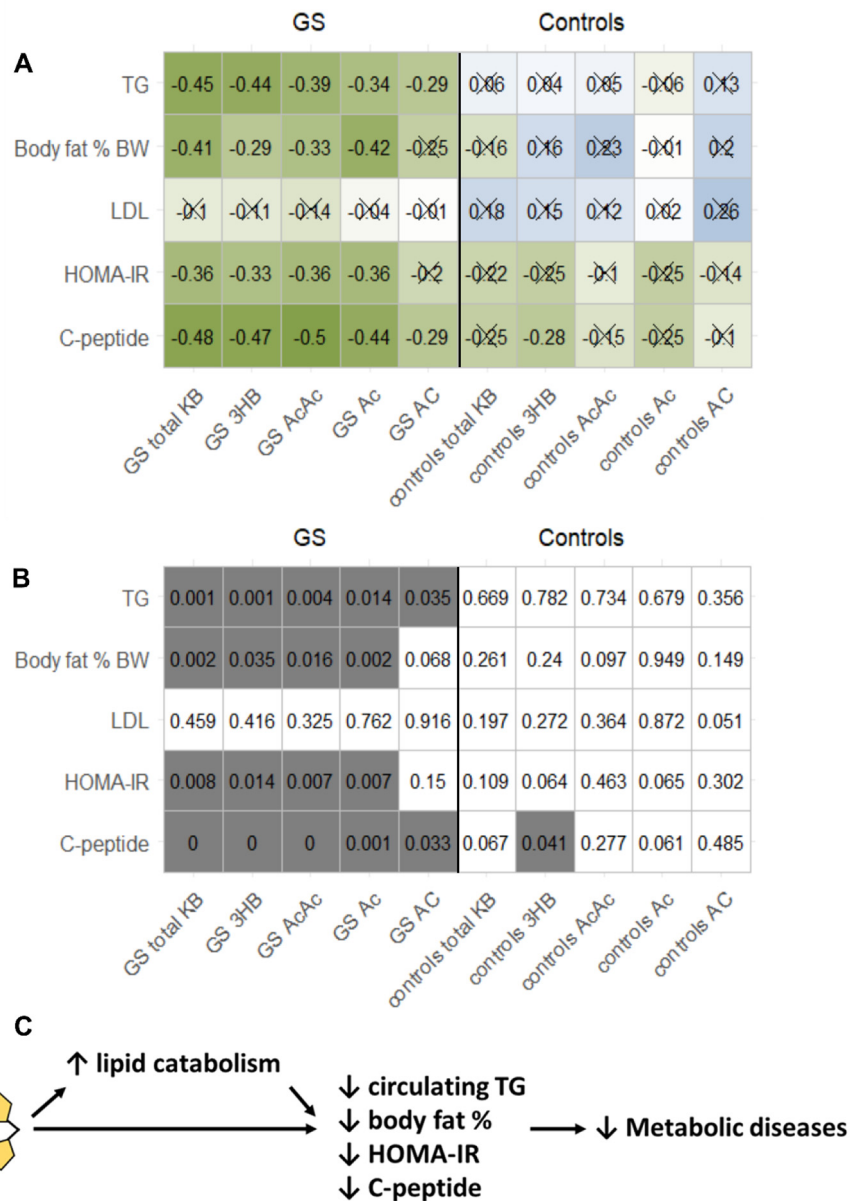


**Fig. 6.** Lipid catabolism and the bilirubin-associated protection against chronic metabolic diseases. (A) Correlation coefficients (r) of major risk factors for DMT2 and CVD with lipid catabolites in the GS and control group. Positive correlations are in blue and negative in green using Pearson or Spearman-Rho. Crosses indicate non-significant correlations ( $p > 0.05$ ). (B) Corresponding p-values,  $0 < p < 0.001$ . (C) A schematic representation proposing lipid catabolism as one potential mechanism for the protection against chronic metabolic diseases in GS individuals.

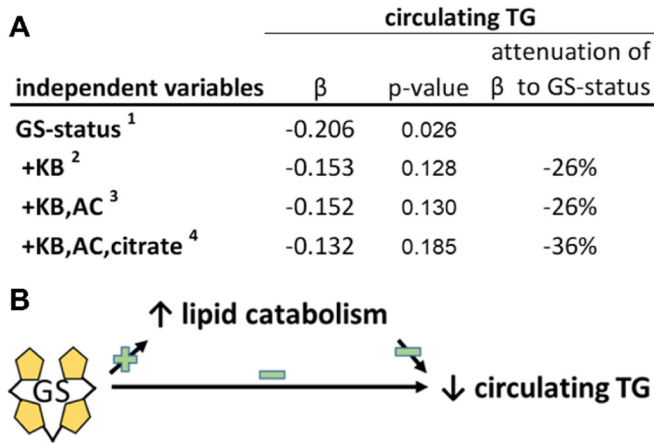


**Fig. 7.** Effect of the GS on circulating TG and mediation through lipid catabolism. (A) Linear regressions were performed to predict circulating TG based on the GS-status 1 and based on the GS-status and lipid catabolism 2, 3, 4. KB, AC, and citrate were used as a measure of lipid catabolism.  $\beta$ : standardised coefficient  $\beta$ ; attenuation of  $\beta$  to GS status: % attenuation of  $\beta$  2, 3, 4 compared to  $\beta$  1. Adjustment for age and gender was not performed due to the age and gender matched study design. (B) A schematic representation of (A) suggesting that the total TG-lowering effect of GS is partially mediated through lipid catabolism.

3.8. Fasting markers and lipid catabolites

Fasting markers such as fasting blood glucose ( $-5\%$ ,  $p = 0.006$ ), insulin ( $-33\%$ ,  $p = 0.002$ ), C-peptide ( $-20\%$ ,  $p = 0.001$ ) and TG

**Table 3**  
TMA metabolism in GS vs controls.

	Gilbert's syndrome		Control		p-Value
TMA	2.13	1.49	1.58	1.22	0.000
TMAO <sup>a</sup>	31.53	10.95	29.70	8.79	0.310
TMAO/TMA <sup>a</sup>	15.88	7.33	21.45	11.01	0.002

The respective concentrations ( $\mu\text{M}$ ) of TMA and TMAO in serum and the TMAO/TMA-ratio are presented as median/IQR or mean/SD<sup>a</sup>.

( $-20\%$ ,  $p = 0.007$ ) were significantly reduced in GS individuals and correlations with KB and AC showed highly significant negative associations only in the GS group (Fig. 8).

3.9. Trimethylamine (TMA) metabolism is altered in GS individuals

TMA is a gut microbial product that is converted to trimethylamine N-oxide (TMAO) in the liver. TMA metabolism has recently emerged as predictor of metabolic diseases [33]. The concentrations of TMA was significantly higher ( $+35\%$ ,  $p < 0.001$ ), of its catabolite trimethylamine N-oxide (TMAO) similar and the TMAO/TMA ratio was significantly lower ( $-26\%$ ,  $p = 0.002$ ) in GS individuals vs. controls (Table 3).

4. Discussion

Protection against CVD and DMT2 in GS individuals has mainly been linked to their favorable lipid phenotype (6, 8, 20), however, underlying

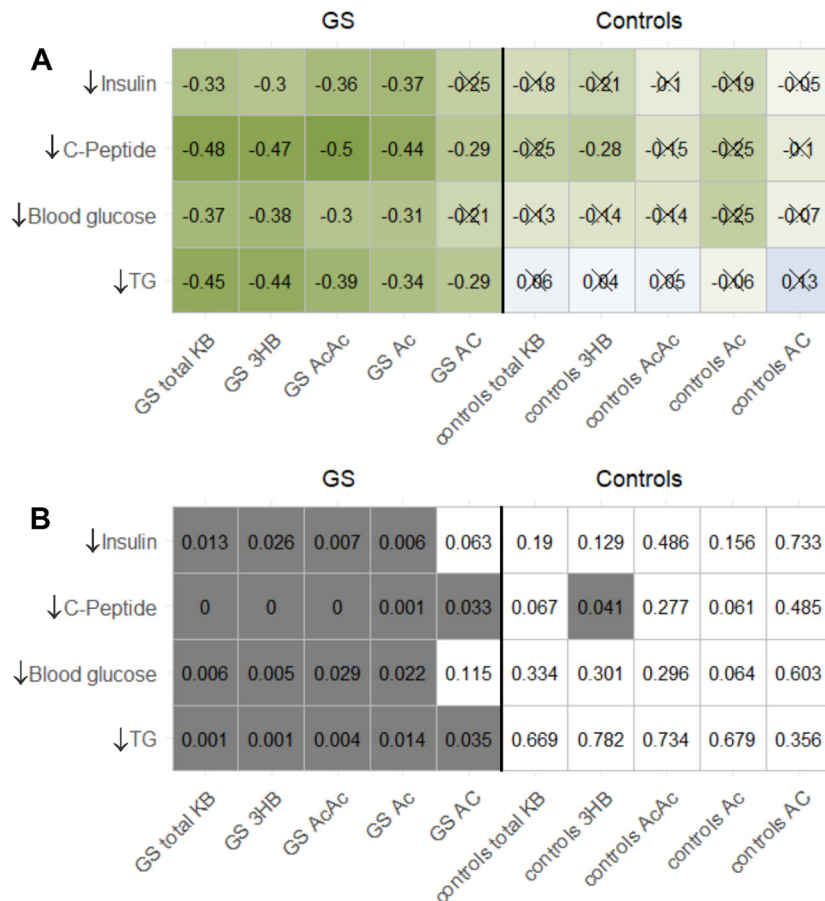


**Fig. 8.** Correlation pattern of typical fasting markers and lipid catabolites in GS and control individuals. (A) Correlation coefficients ( $r$ ) in the GS and control group, arrows indicate the physiological metabolic response to fasting. Positive correlations are in blue and negative in green using Pearson or Spearman-Rho. Crosses indicate non-significant correlations ( $p > 0.05$ ). (B) Corresponding  $p$ -values,  $0 < p < 0.001$ .



mechanistic data remained lacking. We used, for the first time in this context, a metabolomics approach in addition to circulating hormonal and key molecular regulators as supportive biomarkers in a well characterized GS case control study.

Substantially elevated AC, 3HB, AcAc and Ac serum concentrations revealed enhanced FAO and hepatic ketogenesis in GS individuals compared to controls (Table 3). Strong and significant correlations of AC with the three KBs are congruent with ACs and KBs being end products of the FAO and underpin an increased FAO-mediated (based on increased AC) KB production in GS individuals. The metabolomics profile demonstrated additional GS-specific metabolites that are associated with enhanced mitochondrial metabolism. Briefly, citrate and amino acid intermediates were elevated in GS individuals, which was also consistent with a reduction in creatine levels. This was in turn congruent with increased PGC1 $\alpha$  levels in PBMCs of GS individuals (Fig. 4) [22], which is a transcription factor that controls numerous mitochondrial genes responsible for oxidative metabolism and mitochondrial biogenesis [34]. We therefore conclude a GS-specific metabolic shift towards lipid catabolism.

For further confirmation, we investigated molecular regulators and their associations with lipid catabolism. PPAR $\alpha$  and AMPK are stimulators of mitochondrial lipid catabolism [35–37]. Since both are evolutionarily conserved in all eukaryotes [38] and ubiquitously expressed in tissues such as liver and skeletal muscle as well as immune cells [39], we previously analyzed PPAR $\alpha$  (Ser12) and AMPK ( $\alpha$ 1 T183 and  $\alpha$ 2 T172) phosphorylation in PBMCs and found increased activity of both proteins in GS individuals [22]. This is consistent with data from in vitro and in vivo studies reporting UCB as a direct ligand for PPAR $\alpha$  [11,40] and increased hepatic PPAR $\alpha$  activity in mildly hyperbilirubinemic mice [7]. In the present study we explored the relationship between activated PPAR $\alpha$  and AMPK with their downstream metabolites AC and KB and found significant correlations reflecting the stimulatory role of PPAR $\alpha$  and AMPK in lipid catabolism, both increased in GS individuals (Fig. 4). Very recently, Hinds et al. [41] reported similar observations in mice demonstrating increased PPAR $\alpha$  target gene expression of *FATP1/2* and *ACO1* along with increased 3HB blood concentrations in bilirubin-treated mice [41]. Additionally, a very recently published study reported an enhanced PPAR $\alpha$ -mediated mitochondrial function and lipid metabolism in 3T3L1 adipocytes after exposure to biliverdin, the precursor of bilirubin [11]. A further major regulator of lipid catabolism is insulin as it not only stimulates glucose oxidation and lipogenesis but simultaneously inhibits the contribution of FAO to energy supply. Inversely, decreased insulin concentrations observed in GS individuals clear the way for FAO and ketogenesis. Indeed, significant inverse correlations between insulin and lipid catabolites were exclusively observed in the GS group (Fig. 5). In agreement with comparably less insulin, glucagon a hormone that opposes the action of insulin and enhances FAO [42] was significantly correlated to all KB only in GS individuals but remained unchanged between the groups. T3 a potent stimulator of mitochondrial FAO [43] was significantly increased in GS individuals and correlated along with the T3/T4 ratio significantly with AC and KB respectively only in the GS group. THs have previously been associated with bilirubin because they are both glucuronidated by UGT1A1 [44]. Increased UGT activity leads to a depletion of circulating TH. However, similarly to bilirubin, mutations in the *UGT1A1* (such as *UGT1A1\*28* (TA)<sub>6>7</sub> polymorphism) caused a reduced glucuronidation of TH in human liver microsomes and had previously been proposed to play a role in TH homeostasis [44,45]. Thus UGT1A1-mediated TH metabolism might be another underlying mechanism of the bilirubin-associated metabolic health and in this context increased circulating bilirubin would be a marker of a reduced UGT1A1 activity, which is described in GS [46].

Taken together, the GS-associated metabolites as well PPAR $\alpha$ , AMPK, insulin, glucagon and THs reveal a complementary pattern of lipid catabolic conditions in GS individuals. These findings suggest for the first time underlying mechanisms based on PPAR $\alpha$ , AMPK, insulin

and THs associated with an increased lipid catabolism in mildly hyperbilirubinemic subjects.

Lipid catabolism is inversely associated with dyslipidemia and obesity, conditions that drive the pathogenesis of DMT2 and CVD. In agreement with this, we observed highly significant inverse correlations between lipid catabolites and circulating TG, body fat, HOMA-IR and C-peptide exclusively in GS individuals. Furthermore, we found that the total TG-lowering effect of GS is partially mediated through their increased lipid catabolism, which can be considered as a statistical proof of principle. Similar to our observations, bilirubin-treated mice on a high fat diet experienced a reduction in serum TG, hepatic fat mass and body weight along with increased 3HB blood concentrations [41], further emphasizing lipid catabolism to be a key determinant of the bilirubin-associated protection against CVD and DMT2.

The capacity of bilirubin to shape a health beneficial lipid and glucose phenotype has been demonstrated in several other animal models [7,11,47–49] and in vitro studies [40,50]. Numerous large prospective epidemiological studies reported that bilirubin is associated with beneficial characteristics (improved BMI, blood lipids and insulin resistance) and a reduced risk of CVD and DMT2 [9,10,14,15,51–54]. In this context, our metabolomics approach found acetylglycine to be more abundant in GS individuals. Intriguingly, decreased glycine levels have been associated with a higher incidence of CVD and DMT2 [55–57] and a causal genetic relationship of glycine and glycine metabolites such as acetylglycine with CVD and DMT2 risk has been reported [58].

GS individuals exhibited a stronger metabolic response to fasting. As mentioned earlier, AC and KB levels were significantly higher in GS individuals. The same was true for other metabolites including citrate, 2-hydroxybutyric acid, 2-aminobutyric acid, as well as leucine and its ketoacids 2-oxoisocaproate and 3-hydroxyisovalerate (Table 2), all of which have been associated with extended periods of fasting [59,60]. Thus, the metabolomics profile of the GS group mirrors a metabolome of prolonged fasting. These results agree with significantly reduced fasting blood glucose, insulin, C-peptide and TG and their inverse relationship with markers of lipid catabolism (AC, KB) (Fig. 8) indicating a decreased glucose metabolism in favor of lipid catabolism in fasted GS individuals. Increased citrate and pPPAR $\alpha$  levels, observed in GS individuals are consistent with the latter observation as they both have been proposed to diminish glucose oxidation [61,62], in addition to their role in lipid catabolism (discussed above). Overall, our findings imply that GS metabolism handles limited glucose availability through a more efficient switch in energy substrate from glucose towards fatty acids in response to fasting.

Increased TMA serum concentrations as identified in GS can be the result of a diet rich in red meat as well as an increased gut microbial metabolism of carnitine and choline [33]. In our study, both the red meat consumption and the composition of fecal microbiota were similar between GS and control individuals (in press) [63]. However, increased TMA in hand with similar TMAO levels between groups can also be attributable to a lower activity of Flavin-containing monooxygenase 3 (FMO3), the enzyme that catalyzes the TMA to TMAO conversion. This could be a promising target in GS since FMO3 and the bilirubin-specific UGT1A1 are both enzymes of the hepatic drug metabolism susceptible to pharmacological inhibition. FMO3 affects metabolic health and its suppression is described to reduce body fat as well as plasma TG, glucose and insulin concentrations [64]. This phenotype, which shares striking similarity with GS, is proposed to be due to a reduction in Foxo1 levels, a metabolic key node that controls hepatic gluconeogenesis [65,66]. Conversely, increased gluconeogenesis is a crucial feature of insulin resistance and contributes to fasting hyperglycemia [67]. In terms of regulation of gluconeogenesis, similar levels of alanine and lactate (substrates of gluconeogenesis) as well as ALT and LDH (enzymes playing a role in gluconeogenesis that were initially measured to verify absence of liver damage) between GS and control individuals might indicate no alanine or lactate-specific reduced regulation of gluconeogenesis [68,69], which however warrants more detailed

investigation. To the best of our knowledge, a role of FMO3 and TMA metabolism in the bilirubin-associated health beneficial phenotype has not been proposed so far. However, this finding would explain the favorable glucose profile in GS as well as the observed shift in energy substrate. We therefore suggest to investigate the role of FMO3 in GS.

This study is of an observational nature, therefore no causality can be inferred. A further limitation of this study is that we did not have access to tissue of GS individuals such as liver or skeletal muscle. Measurements of AMPK, PPAR $\alpha$  and further aspects of mitochondrial regulation could be performed to ultimately confirm mitochondrial FAO in metabolically active tissue of GS individuals. In addition to lipid catabolism, the role of adipose tissue and lipolysis in the metabolic protection of GS individuals should be investigated in future.

## 5. Conclusion

We showed an enhanced lipid catabolism in GS individuals supported by increased PPAR $\alpha$ , AMPK and TH as well as decreased insulin levels. We further showed that lipid catabolism partially mediates the favorable lipid phenotype (lower TG) of GS. Thus, the enhanced lipid catabolism in GS seems to be the key strategy in the protective role of bilirubin against obesity, dyslipidemia, DMT2 and CVD and warrants further clinical evaluation especially in obese and dyslipidemic patients.

Supplementary data to this article can be found online at <https://doi.org/10.1016/j.metabol.2021.154913>.

## Funding

Fonds zur Förderung der wissenschaftlichen Forschung (FWF) Stand-Alone Project grant, P 29608 (KHW).

## CRediT authorship contribution statement

CAH contributed to the NMR analysis, performed the data analysis, interpreted the data, designed the graphs and wrote the manuscript.

KHW designed and supervised the project and revised the manuscript.

CM and MHW conducted the human study and revised the manuscript.

LVT performed the NMR analysis.

AAM provided the metabolomics facilities, supervised the NMR analysis and the statistical analysis of NMR data, contributed with data interpretation and revised the manuscript.

E.M. supervised the NMR analysis and the NMR statistical analysis.

BF and PAZ contributed to the manuscript with intellectual importance and revised the manuscript.

ACB contributed to the initial conceptualization of the human study and revised the manuscript.

AT was supportive with R data analysis.

DD was study physician and provided together with R.M. the facilities of the Clinical Institute of Laboratory Medicine and the Department of Clinical Pharmacology.

HF supervised the mediation analysis and revised the manuscript.

## Declaration of competing interest

None, the authors have declared that no conflict of interest exists.

## Acknowledgments

We are grateful to Univ.-Prof. i.R. Dr. Hans Goldenberg for discussions and advice regarding biochemical aspects of data interpretation.

“Where authors are identified as personnel of the International Agency for Research on Cancer/World Health Organization, the authors alone are responsible for the views expressed in this article and they do

not necessarily represent the decisions, policy or views of the International Agency for Research on Cancer/World Health Organization.”

## References

- [1] Vos T, Allen C, Arora M, Barber RM, Bhutta ZA, Brown A, et al. Global, regional, and national incidence, prevalence, and years lived with disability for 310 diseases and injuries, 1990–2015: a systematic analysis for the Global Burden of Disease Study 2015. *Lancet*. 2016;388:1545–602.
- [2] Després J-P. Body fat distribution and risk of cardiovascular disease: an update. *Circulation*. 2012;126:1301–13.
- [3] Vos T, Abajobir AA, Abate KH, Abbafati C, Abbas KM, Abd-Allah F, et al. Global, regional, and national incidence, prevalence, and years lived with disability for 328 diseases and injuries for 195 countries, 1990–2016: a systematic analysis for the Global Burden of Disease Study 2016. *Lancet*. 2017;390:1211–59.
- [4] Lyssenko V, Jonsson A, Almgren P, Pulizzi N, Isomaa B, Tuomi T, et al. Clinical risk factors, DNA variants, and the development of type 2 diabetes. *N Engl J Med*. 2008;359:2220–32.
- [5] Semenkovich CF. Insulin resistance and atherosclerosis. *J Clin Invest*. 2006;116:1813–22.
- [6] Bulmer A, Verkade H, Wagner K-H. Bilirubin and beyond: a review of lipid status in Gilbert's syndrome and its relevance to cardiovascular disease protection. *Prog Lipid Res*. 2013;52:193–205.
- [7] Hinds Jr TD, Hosick PA, Chen S, Tukey RH, Hankins MW, Nestor-Kalinowski A, et al. Mice with hyperbilirubinemia due to Gilbert's syndrome polymorphism are resistant to hepatic steatosis by decreased serine 73 phosphorylation of PPAR $\alpha$ . *Am J Physiol Endocrinol Metab*. 2017;312:E244–52.
- [8] Hamoud A-R, Weaver L, Stec DE, Hinds TD. Bilirubin in the liver–gut signaling axis. *Trends Endocrinol Metab*. 2018;29:140–50.
- [9] Riphagen IJ, Deetman PE, Bakker SJ, Navis G, Cooper ME, Lewis JB, et al. Bilirubin and progression of nephropathy in type 2 diabetes: a post hoc analysis of RENAAL with independent replication in IDNT. *Diabetes*. 2014;63:2845–53.
- [10] Kimm H, Yun JE, Jo J, Jee SH. Low serum bilirubin level as an independent predictor of stroke incidence: a prospective study in Korean men and women. *Stroke*. 2009;40:3422–7.
- [11] Gordon DM, Neifer KL, Hamoud A-RA, Hawk CF, Nestor-Kalinowski AL, Miruzzi SA, et al. Bilirubin remodels murine white adipose tissue by reshaping mitochondrial activity and the coregulator profile of peroxisome proliferator-activated receptor  $\alpha$ . *J Biol Chem*. 2020;295(29):9804–22. <https://doi.org/10.1074/jbc.RA120.013700>.
- [12] Lin J-P, Vitek L, Schwertner HA. Serum bilirubin and genes controlling bilirubin concentrations as biomarkers for cardiovascular disease. *Clin Chem*. 2010;56:1535–43.
- [13] Abbasi A, Deetman PE, Corpeleijn E, Gansevoort RT, Gans RO, Hillege HL, et al. Bilirubin as a potential causal factor in type 2 diabetes risk: a Mendelian randomization study. *Diabetes*. 2015;64:1459–69.
- [14] Stender S, Frikke-Schmidt R, Nordestgaard BG, Grande P, Tybjaerg-Hansen A. Genetically elevated bilirubin and risk of ischaemic heart disease: three Mendelian randomization studies and a meta-analysis. *J Intern Med*. 2013;273:59–68.
- [15] Horsfall LJ, Nazareth I, Petersen I. Cardiovascular events as a function of serum bilirubin levels in a large, statin-treated cohort. *Circulation*. 2012;126:2556–64.
- [16] Nano J, Muka T, Cepeda M, Voortman T, Dhana K, Brahimaj A, et al. Association of circulating total bilirubin with the metabolic syndrome and type 2 diabetes: a systematic review and meta-analysis of observational evidence. *Diabetes Metab*. 2016;42:389–97.
- [17] Wagner K-H, Shiels RG, Lang CA, Seyed Khoei N, Bulmer AC. Diagnostic criteria and contributors to Gilbert's syndrome. *Crit Rev Clin Lab Sci*. 2018;55:129–39.
- [18] Bosma PJ, Chowdhury JR, Bakker C, Gantla S, de Boer A, Oostra BA, et al. The genetic basis of the reduced expression of bilirubin UDP-glucuronosyltransferase 1 in Gilbert's syndrome. *N Engl J Med*. 1995;333:1171–5.
- [19] Monaghan G, Ryan M, Hume R, Burchell B, Seddon R. Genetic variation in bilirubin UDP-glucuronosyltransferase gene promoter and Gilbert's syndrome. *Lancet*. 1996;347:578–81.
- [20] Wallner M, Marculescu R, Doberer D, Wolzt M, Wagner O, Vitek L, et al. Protection from age-related increase in lipid biomarkers and inflammation contributes to cardiovascular protection in Gilbert's syndrome. *Clin Sci*. 2013;125:257–64.
- [21] Khoei NS, Grindel A, Wallner M, Mölzer C, Doberer D, Marculescu R, et al. Mild hyperbilirubinaemia as an endogenous mitigator of overweight and obesity: implications for improved metabolic health. *Atherosclerosis*. 2018;269:306–11.
- [22] Mölzer C, Wallner M, Kern C, Tosevska A, Schwarz U, Zadnikar R, et al. Features of an altered AMPK metabolic pathway in Gilbert's syndrome, and its role in metabolic health. *Sci Rep*. 2016;6:30051.
- [23] Wallner M, Antl N, Rittmannsberger B, Schreidl S, Najafi K, Müllner E, et al. Antigenotoxic potential of bilirubin in vivo: damage to DNA in hyperbilirubinemic human and animal models. *Cancer Prevent Res (Philadelphia, Pa)*. 2013;6:1056–63.
- [24] Wallner M, Bulmer AC, Mölzer C, Müllner E, Marculescu R, Doberer D, et al. Haem catabolism: a novel modulator of inflammation in Gilbert's syndrome. *Eur J Clin Invest*. 2013;43:912–9.
- [25] von Ahnen N, Oellerich M, Schutz E. DNA base bulge vs unmatched end formation in probe-based diagnostic insertion/deletion genotyping: genotyping the UGT1A1 (TA) $_n$  polymorphism by real-time fluorescence PCR. *Clin Chem*. 2000;46:1939–45.
- [26] Moazzami AA, Zhang J-X, Kamal-Eldin A, Aman P, Hallmans G, Johansson J-E, et al. Nuclear magnetic resonance-based metabolomics enable detection of the effects of a whole grain rye and rye bran diet on the metabolic profile of plasma in prostate cancer patients. *J Nutr*. 2011;141:2126–32.

- [27] Röhnisch HE, Eriksson J, Müllner E, Agback P, Sandström C, Moazzami AA. AQUA: an automated quantification algorithm for high-throughput NMR-based metabolomics and its application in human plasma. *Anal Chem.* 2018;90:2095–102.
- [28] Storey JD. A direct approach to false discovery rates. *J R Stat Soc Ser B (Stat Methodol).* 2002;64:479–98.
- [29] Kadakol A, Ghosh SS, Sappal BS, Sharma G, Chowdhury JR, Chowdhury NR. Genetic lesions of bilirubin uridine-diphosphoglucuronate glucuronosyltransferase (UGT1A1) causing Crigler-Najjar and Gilbert syndromes: correlation of genotype to phenotype. *Hum Mutat.* 2000;16:297–306.
- [30] Owen OE, Kalhan SC, Hanson RW. The key role of anaplerosis and cataplerosis for citric acid cycle function. *J Biol Chem.* 2002;277:30409–12.
- [31] Nordestgaard BG, Varbo A. Triglycerides and cardiovascular disease. *Lancet.* 2014;384:626–35.
- [32] Yusuf S, Joseph P, Rangarajan S, Islam S, Mentz A, Hystad P, et al. Modifiable risk factors, cardiovascular disease, and mortality in 155 722 individuals from 21 high-income, middle-income, and low-income countries (PURE): a prospective cohort study. *Lancet.* 2020;395:795–808.
- [33] Koeth RA, Wang Z, Levison BS, Buffa JA, Org E, Sheehy BT, et al. Intestinal microbiota metabolism of L-carnitine, a nutrient in red meat, promotes atherosclerosis. *Nat Med.* 2013;19:576–85.
- [34] Austin S, St-Pierre J. PGC1 $\alpha$  and mitochondrial metabolism—emerging concepts and relevance in ageing and neurodegenerative disorders. *J Cell Sci.* 2012;125:4963–71.
- [35] Kersten S, Seydoux J, Peters JM, Gonzalez FJ, Desvergne B, Wahli W. Peroxisome proliferator-activated receptor  $\alpha$  mediates the adaptive response to fasting. *J Clin Invest.* 1999;103:1489–98.
- [36] Towler MC, Hardie DG. AMP-activated protein kinase in metabolic control and insulin signaling. *Circ Res.* 2007;100:328–41.
- [37] Bouzakri K, Austin R, Rune A, Lassman ME, Garcia-Roves PM, Berger JP, et al. Malonyl CoenzymeA decarboxylase regulates lipid and glucose metabolism in human skeletal muscle. *Diabetes.* 2008;57:1508–16.
- [38] Takada I, Yu RT, Xu HE, Lambert MH, Montana VG, Kliewer SA, et al. Alteration of a single amino acid in peroxisome proliferator-activated receptor- $\alpha$  (PPAR $\alpha$ ) generates a PPAR $\delta$  phenotype. *Mol Endocrinol.* 2000;14:733–40.
- [39] Chinetti G, Lestavel S, Bocher V, Remaley AT, Neve B, Torra IP, et al. PPAR- $\alpha$  and PPAR- $\gamma$  activators induce cholesterol removal from human macrophage foam cells through stimulation of the ABCA1 pathway. *Nat Med.* 2001;7:53–8.
- [40] Stec DE, John K, Trabbic CJ, Luniwal A, Hankins MW, Baum J, et al. Bilirubin binding to PPAR $\alpha$  inhibits lipid accumulation. *PLoS One.* 2016;11:e0153427.
- [41] Hinds TD, Creeden JF, Gordon DM, Stec DF, Donald MC, Stec DE. Bilirubin nanoparticles reduce diet-induced hepatic steatosis, improve fat utilization, and increase plasma  $\beta$ -hydroxybutyrate. *Front Pharmacol.* 2020;11.
- [42] Longuet C, Sinclair EM, Maida A, Baggio LL, Maziarz M, Charron MJ, et al. The glucagon receptor is required for the adaptive metabolic response to fasting. *Cell Metab.* 2008;8:359–71.
- [43] Mullur R, Liu Y-Y, Brent GA. Thyroid hormone regulation of metabolism. *Physiol Rev.* 2014;94:355–82.
- [44] Graber ALY, Ramirez J, Innocenti F, Ratain MJ. UGT1A1\* 28 genotype affects the in-vitro glucuronidation of thyroxine in human livers. *Pharmacogenet Genomics.* 2007;17:619–27.
- [45] Findlay KAB, Kaptein E, Visser TJ, Burchell B. Characterization of the uridine diphosphate-glucuronosyltransferase-catalyzing thyroid hormone glucuronidation in Man1. *J Clin Endocrinol Metab.* 2000;85:2879–83.
- [46] Hirschfield G, Alexander G. Gilbert's syndrome: an overview for clinical biochemists. *Ann Clin Biochem.* 2006;43:340–3.
- [47] Liu J, Dong H, Zhang Y, Cao M, Song L, Pan Q, et al. Bilirubin increases insulin sensitivity by regulating cholesterol metabolism, adipokines and PPAR $\gamma$  levels. *Sci Rep.* 2015;5:9886.
- [48] Dong H, Huang H, Yun X, Kim D-S, Yue Y, Wu H, et al. Bilirubin increases insulin sensitivity in leptin-receptor deficient and diet-induced obese mice through suppression of ER stress and chronic inflammation. *Endocrinology.* 2014;155:818–28.
- [49] Vidimic J, Pillay J, Shrestha N, Dong L-F, Neuzil J, Wagner K-H, et al. Mitochondrial function, fatty acid metabolism, and body composition in the hyperbilirubinemic Gunn rat. *Front Pharmacol.* 2021;12:73.
- [50] Hana CA, Klebermass E-M, Balber T, Mitterhauser M, Quint R, Hirtl Y, et al. Inhibition of lipid accumulation in skeletal muscle and liver cells: a protective mechanism of bilirubin against diabetes mellitus type 2. *Front Pharmacol.* 2020;11:2329.
- [51] Kunutsor SK, Kieneker LM, Burgess S, Bakker SJ, Dullaart RP. Circulating total bilirubin and future risk of hypertension in the general population: the prevention of renal and vascular end-stage disease (PREVEND) prospective study and a Mendelian randomization approach. *J Am Heart Assoc.* 2017;6:e006503.
- [52] Kunutsor SK, Bakker SJ, Gansevoort RT, Chowdhury R, Dullaart RP. Circulating total bilirubin and risk of incident cardiovascular disease in the general population. *Arterioscler Thromb Vasc Biol.* 2015;35:716–24.
- [53] Mahabadi AA, Lehmann N, Möhlenkamp S, Kälsch H, Bauer M, Schulz R, et al. Association of bilirubin with coronary artery calcification and cardiovascular events in the general population without known liver disease: the Heinz Nixdorf Recall study. *Clin Res Cardiol.* 2014;103:647–53.
- [54] Troughton JA, Woodside JV, Young IS, Arveiler D, Amouyel P, Ferrières J, et al. Bilirubin and coronary heart disease risk in the Prospective Epidemiological Study of Myocardial Infarction (PRIME). *Eur J Prev Cardiol.* 2007;14:79–84.
- [55] Ding Y, Svingen GF, Pedersen ER, Gregory JF, Ueland PM, Tell GS, et al. Plasma glycine and risk of acute myocardial infarction in patients with suspected stable angina pectoris. *J Am Heart Assoc.* 2015;5:e002621.
- [56] Floegel A, Stefan N, Yu Z, Mühlenbruch K, Drogan D, Joost H-G, et al. Identification of serum metabolites associated with risk of type 2 diabetes using a targeted metabolomic approach. *Diabetes.* 2013;62:639–48.
- [57] Merino J, Leong A, Liu C-T, Porneala B, Walford GA, von Grotthuss M, et al. Metabolomics insights into early type 2 diabetes pathogenesis and detection in individuals with normal fasting glucose. *Diabetologia.* 2018;61:1315–24.
- [58] Wittemans LBL, Lotta LA, Oliver-Williams S, Stewart ID, Surendran P, Karthikeyan S, et al. Assessing the causal association of glycine with risk of cardio-metabolic diseases. *Nat Commun.* 2019;10:1060.
- [59] Rubio-Aliaga I, de Roos B, Duthie SJ, Crosley LK, Mayer C, Horgan G, et al. Metabolomics of prolonged fasting in humans reveals new catabolic markers. *Metabolomics.* 2011;7:375–87.
- [60] Krug S, Kastenmüller G, Stückler F, Rist MJ, Skurk T, Sailer M, et al. The dynamic range of the human metabolome revealed by challenges. *FASEB J.* 2012;26:2607–19.
- [61] Garland P, Randle P, Newsholme E. Citrate as an intermediary in the inhibition of phosphofructokinase in rat heart muscle by fatty acids, ketone bodies, pyruvate, diabetes and starvation. *Nature.* 1963;200:169–70.
- [62] Hue L, Taegtmeyer H. The Randle cycle revisited: a new head for an old hat. *Am J Physiol Endocrinol Metab.* 2009;297:E578–91.
- [63] Zöhrer PA, Hana CA, Khoei NS, Mölzer C, Hörmann-Wallner M, Tosevska A, et al. Gilbert's syndrome and the gut microbiota – Insights from the case-control BILLIHEALTH study. *Front Cell Infect Microbiol Microbiome Health Dis.* 2021. <https://doi.org/10.3389/fcimb.2021.701109>.
- [64] Shih DM, Wang Z, Lee R, Meng Y, Che N, Charugundla S, et al. Flavin containing monooxygenase 3 exerts broad effects on glucose and lipid metabolism and atherosclerosis. *J Lipid Res.* 2015;56:22–37.
- [65] Miao J, Ling AV, Manthena PV, Gearing ME, Graham MJ, Crooke RM, et al. Flavin-containing monooxygenase 3 as a potential player in diabetes-associated atherosclerosis. *Nat Commun.* 2015;6:1–10.
- [66] Chen S, Henderson A, Petriello MC, Romano KA, Gearing M, Miao J, et al. Trimethylamine N-oxide binds and activates PERK to promote metabolic dysfunction. *Cell Metab.* 2019;30:1141–51 [e5].
- [67] Bock G, Chittilapilly E, Basu R, Toffolo G, Cobelli C, Chandramouli V, et al. Contribution of hepatic and extrahepatic insulin resistance to the pathogenesis of impaired fasting glucose: role of increased rates of gluconeogenesis. *Diabetes.* 2007;56:1703–11.
- [68] Gray Lawrence R, Sultana Mst R, Rauckhorst Adam J, Oonthonpan L, Tompkins Sean C, Sharma A, et al. Hepatic mitochondrial pyruvate carrier 1 is required for efficient regulation of gluconeogenesis and whole-body glucose homeostasis. *Cell Metab.* 2015;22:669–81.
- [69] Okun JG, Rusu PM, Chan AY, Wu Y, Yap YW, Sharkie T, et al. Liver alanine catabolism promotes skeletal muscle atrophy and hyperglycaemia in type 2 diabetes. *Nat Metab.* 2021;3:394–409.